研 究 速 報

SEM-AFM for 3 D Nano-Structure Measurement

Kimitake FUKUSHIMA*, Daisuke SAYA* and Hideki KAWAKATSU*

1. Introduction

Through recent advancements in silicon micromachining techniques, various types of three-dimensional MEMS (Micro Electro Mechanical System) or NEMS (Nano-EMS) structures are being made. Although these structures are said to have high structural strength compared to macroscopic structures, visualization or measurement of mechanical characteristics are left to be done due to lack of appropriate measurement tool.

Atomic force microscope (AFM)[1] which was originally invented as a tool for measuring surface profile and properties, has recently come to be used as a tool for measuring mechanical characteristics of structures fabricated by MEMS technology.[2–4] By pressing the AFM cantilever against the sample and measuring the ratio between the deflection of the cantilever of the AFM and the deflection of the sample pressed by the AFM, spring constant of the sample is calculated. Although this method is applicable to structures with relatively large surface area, AFM measurement of three-dimensional or nanometric structures were difficult due to lack of visual aid for tip positioning. Since the maximum resolution of an optical microscope used for AFM tip positioning is limited by diffraction limit to about 1μm (Fig. 1), exact point or direction of contact could never be known.

Usage of a combined scanning electron microscope (SEM)-AFM system would solve this problem. However, existing SEM-AFM systems are usually just a SEM and a AFM targeted at the same sample without the capability of simultaneous SEM and AFM operation[5–8].

As a solution to this problem, we have developed a new versatile SEM-AFM system that consists of a SEM and a detachable AFM module capable of easy sample change and adjustment in and outside the SEM[9]. In this paper, we will report on the basic setup and the results of experiments done by the SEM-AFM system.

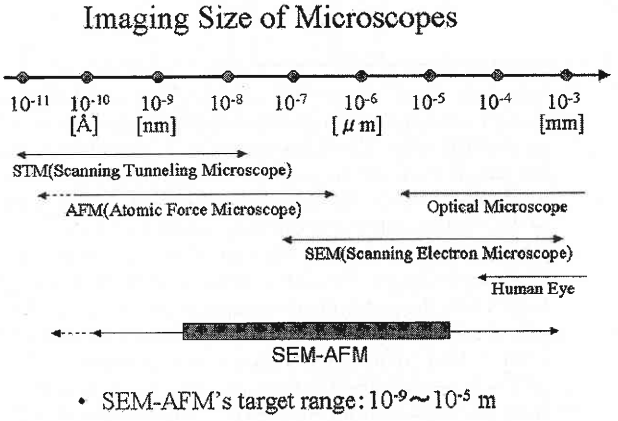

Fig. 1 Operational scale of various microscopes.

2. Description of the SEM-AFM System

The SEM-AFM is made by attaching an AFM module onto the stage of a SEM. The SEM used is a commercially available SEM with a tungsten filament as a hot electron source.[10] A schematic figure of the removable AFM module is shown in Figure 1. The AFM module has a size of 10 cm by 10 cm and a height under 36 mm. The height of the AFM module is kept low and the distance from the highest point of the AFM module to the sample is kept under 5mm to realize a short working distance from the SEM electron beam outlet to the sample, thus creating a high resolution SEM image. The operational working distance lies between 6 to 30 mm. The SEM viewing angle is from 0 to 10 degrees in terms of angle of attack (AOA) against the sample surface. A higher AOA can be achieved by attaching a block between the AFM module and the SEM stage. The path from the sample to the secondary

*Center for International Research on Micro-Mechatronics, Institute of Industrial Science, The University of Tokyo.

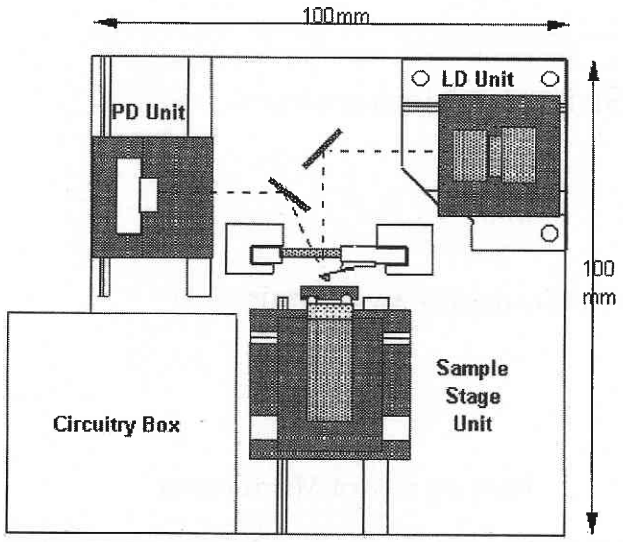

Fig. 2 Schematic figure of the AFM module. The AFM utilizes a conventional optical lever method. The module is mounted on the SEM stage. The SEM electron beam is irradiated onto the sample from the near side. The height of the module is kept under 36 mm and the distance from the highest point of the AFM module to the cantilever tip under 5 mm to realize a low working distance from the SEM beam source and thus a clear image. This also enables variable SEM viewing angles. Also the path from the sample to the secondary electron detector is kept clear. The sample stage is equipped with a three DOF remote controlled coarse actuator and an AFM scanner. PD and LD bases are also equipped with a 1 DOF coarse actuator for adjustment of the optical path within the SEM vacuum chamber.

electron collector is kept open for obtaining sharp SEM image. The AFM module consists of a sample stage, a PD unit, a LD unit, a cantilever holder mount, and a circuitry box. For AFM operation, conventional optical lever method11)is used to measure the cantilever deflection.

The sample stage is equipped with six shear force piezos and one tube piezo with five electrodes. By utilizing an inertia drive method,[12–17] these piezos comprise a three-degree-of-freedom (DOF) coarse actuator with nanometer resolution. The tube piezo also acts as a scanner of AFM. By combining these piezos, three DOF positioning with sub-angstrom resolution is realized. All of the actuators are controlled remotely from a console outside of the SEM. LD and PD units are both equipped with 1 DOF remote controlled actuator for adjustment of optical lever to compensate for the deflection of the AFM cantilever during evacuation of the SEM chamber. The pre-amplifier is placed inside the circuitry box close to the PD to achieve a high signal-to-noise ratio and protection from the electron beam.

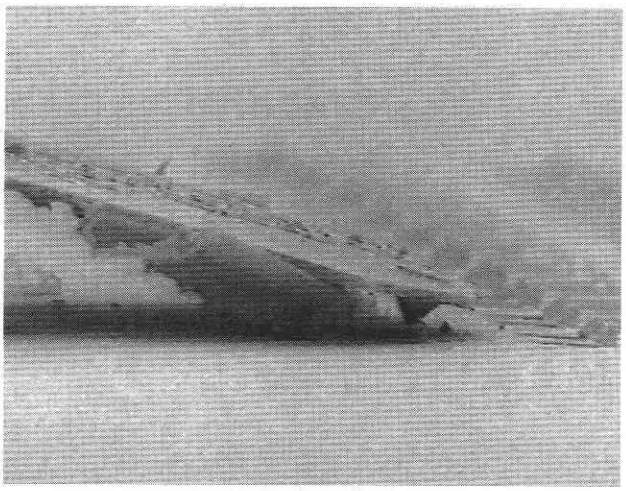

Fig. 3 SEM images of a non-conductive cantilever after contact with sample surface. Probably due to charge-up, particles from unknown sources gathered on the cantilever.

The operation procedures are as follows. First, the sample is fixed to the sample stage. After adjusting the positions of the PD and the LD to form an optical lever, the AFM module is mounted on the SEM stage. Next, air in the SEM chamber is evacuated and the SEM is activated. Since the cantilever deflects from its original position as air and humidity are evacuated, the positions of the LD and the PD are corrected before and after evacuation.

The cantilever used in the SEM-AFM must be either conductive or perfectly coated with conductive materials to avoid charge up resulting from electron beam irradiation. Figure 3 depicts a partially gold-coated non-conductive cantilever after contact with sample surface. Contaminants from unknown sources were attracted to the cantilever because of charge-up.

3. Measurement of 3D nano-structures

Figure 4 depicts a SEM image taken by the SEM-AFM system. The shadowing effect is caused by the AFM cantilever, which prevents some of the secondary electrons originating from the shadowed area from reaching the detector, thus causing a shadow. Since this shadowlike effect occurs as if there was a light source at the secondary electron collector, this effect can be used to determine the distance between the tip and the sample.

Figure 5 (a) to (d) show images taken during the experiment to measure the spring constant of the nano-cantilever. First, we measured the force distance curve (sample deflection distance vs. cantilever deflection = force) at the base of the cantilever, which is rigid to the base of the sample (a). The gradient of this curve (b) was calculated to be 0.21 V/nm. Next we measured the force dis-

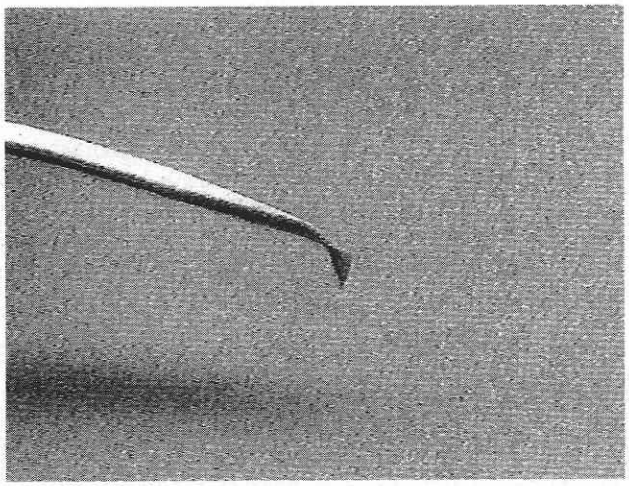

Fig. 4 SEM image obtained with SEM-AFM system. A shadowlike effect is seen due to the blockade of secondary electron path by the cantilever.

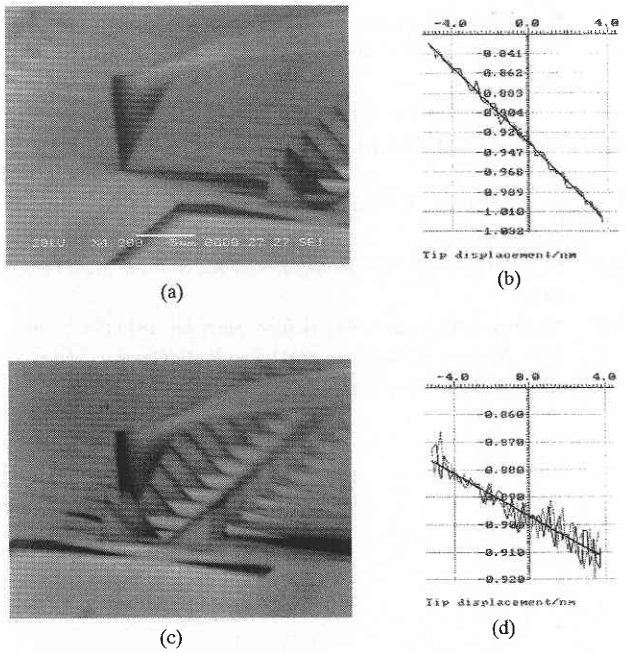

Fig. 5 Images taken during spring constant measurement. By comparing the force curve (b) obtained at the base (a) and (d) at the end of sample (c), spring constant of the sample can be calculated.

tance curve at the end of the nano-cantilever. The gradient was 0.038 V/nm. Since the spring constant of the AFM cantilever used to press the sample was 18-25 N/m, the spring constant of the sample is calculated to be 3-5 N/m.

The shape of the AFM tip of the SEM-AFM system can be modified by irradiating the same spot for a few minutes by the electron beam of the SEM, and accumulating hydrocarbon contaminants within the SEM chamber.[18] For example, the tip of the cantilever can be made into a hook. The shape of the hook can be modified by gradually moving the beam spot toward the desired direction. Also, the tip and the sample can be glued together by irradiating the contact spot between the tip and the sample. These operations can realize the measurement of pull force on small structures as shown in Figure 6.

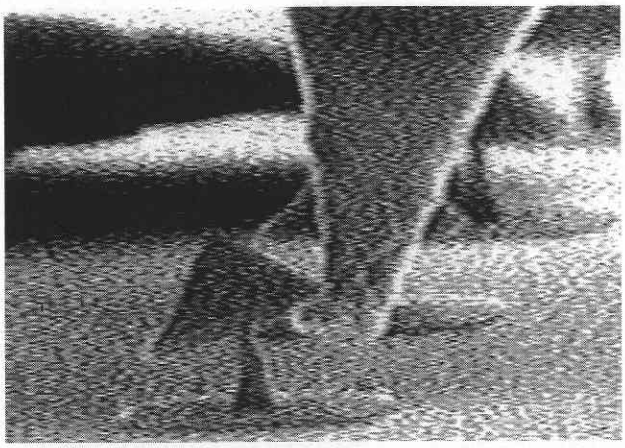

Fig. 6 SEM image of pull up experiment conducted by the nano-hook. The hook is made by irradiating the tip of the cantilever for a few minutes by the electron beam of the SEM, and accumulating hydrocarbon contaminants within the SEM chamber onto the beam spot. By moving the spot gradually toward the end of the hook, a hook of desired shape can be made.

4. Other uses of SEM-AFM

Apart from being used as a tool for measuring 3D nano-structures, SEM-AFM has the capability of a conventional contact mode AFM. A topographical image of gold corrugations on silicon surface taken by the SEM-AFM is shown in Figure 7.

The SEM-AFM system can also have different applications other than AFM. For example, by replacing the cantilever with a cutting tool, or a diamond probe oscillating at ultrasonic frequency, the SEM-AFM system can be used as a sub-micrometer cutting tool with a visual aid. By using this setup, the micrometrical cutting phenomena can be observed in real time.

5. Conclusion

We have developed a versatile SEM-AFM system for measurement of three dimensional nanometric structures. The system consists of a SEM and a removable AFM unit that fits on the SEM stage. The sample stage of the AFM module is equipped with

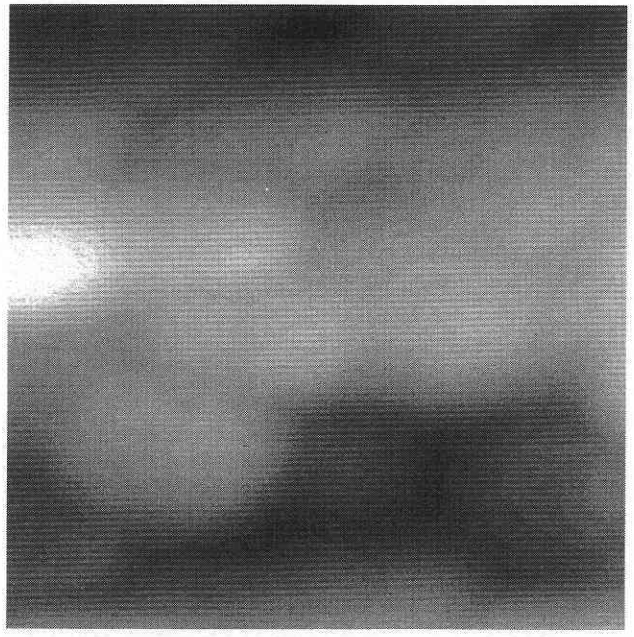

Fig. 7 A topographical image of gold corrugation on silicon surface taken by SEM-AFM (100 nm × 100 nm).

remote controlled piezoelectric actuators enabling three degree of freedom positioning with sub-nanometer resolution and millimeter range under SEM observation. The SEM-AFM system can also be used as a conventional AFM for measurement of surface profile.

(Manuscript received, December 13, 2000)

Acknowledgements

The authors thank Mr. Katsuhito Gotou of Sanyu Denshi and former graduate student Mr. Satoshi Fukuda for technical support on the SEM-AFM.

References

1) G. Binnig, C. Gerber and C. F. Quate: Phys. Rev. Lett. **56** (1986) 930.
2) B. T. Comella and M. R. Scanlon: J. Mat. Sci. **35** (2000) 567.
3) N. A. Burnham, G. Gremaud, A. J. Kulik, P.-J. Gallo, and F. Oulevey: J. Vac. Sci.&Technol. **B14** (1996) 1308.
4) Akihito Torii, Minoru Sasaki, Kazuhiro Hane, and Shigeru Okuma: Meas. Sci. Technol. **7** (1996) 179.
5) A. V. Ermakov and E. L. Garfunkel: Rev. Sci. Instrum. **65** (1994) 2853.
6) A. Kikukawa, S. Hosaka, Y. Honda, and H. Koyanagi: J. Vac. Sci. A **11** (1993) 3092.
7) U. Stahl, C. W. Yuan, and A. L. de Lozanne: Appl. Phys. Lett. **65** (1994) 2878.
8) M. Troyon, H. N. Lei, Z. H. Wang, G. Y. Shang: Microscopy Microanalysis Microstructures **8** (1997) 393.
9) Kimitake Fukushima, Daisuke Saya, and Hideki Kawakatsu: Jpn. J. Appl. Phys. **39** (2000) 3747.
10) JSM-5600LV, JEOL, Tokyo, Japan.
11) G. Meyer and N. M. Amer: Appl. Phys. Lett. **53** (1998) 1045.
12) H. Kawakatsu and T. Higuchi: J. Vac. Sci.&Technol. **A8** (1990) 319.
13) D. W. Pohl: Rev. Sci. Instrum.: **58** (1987) 54.
14) B. W. Corb, M. Ringger, and H.-J. Güntherodt: J. Appl. Phys. **58** (1985) 3947.
15) Ph. Niedermann, R. Emch, and P. Descouts: Rev. Sci. Instrum. **59** (1988) 368.
16) G. W. Stupian and M. S. Leung: J. Vac. Sci. & Technol. **A7** (1989) 2895.
17) M. Anders, M. Thaer and C. Heiden: Surf. Sci. **181** (1987) 176.
18) D. A. Walters, D. Hampton, B. Drake, H. G. Hansma, and P. K. Hansma: Appl. Phys. Lett. **65** (1994) 787.